Plant Nano Biology 6 (2023) 100050

Contents lists available at ScienceDirect

Plant Nano Biology

journal homepage: www.journals.elsevier.com/plant-nano-biology

Bio-synthesized calcium carbonate ($CaCO_3$) nanoparticles: Their anti-fungal properties and application as nanofertilizer on *Lycopersicon esculentum* growth and gas exchange measurements

Thobo Motlhalamme[a,c,*], Hamza Mohamed[a,b,d], Amani Gabriel Kaningini[a,c], Garland Kgosi More[e], Force Tefo Thema[a,b,f], Keletso Cecilia Mohale[c], Malik Maaza[a,b,d]

[a] *UNESCO-UNISA Africa Chair in Nanosciences and Nanotechnology, College of Graduates Studies, University of South Africa, Muckleneuk Ridge, Pretoria 392, South Africa*

[b] *Nanosciences African Network (NANOAFNET), iThemba LABS-National Research Foundation, 1 Old Faure Road, Somerset West 7129, PO Box 722, Somerset West, Western Cape 722, South Africa*

[c] *Department of Agriculture and Animal Health, College of Agriculture and Environmental Sciences, University of South Africa, Private Bag X6, Florida 1710, South Africa*

[d] *iThemba Laboratory for Accelerator-Based Sciences, National Research Foundation, PO Box 722, Somerset West 7129, South Africa*

[e] *College of Agriculture and Environmental Sciences, CAES Laboratories, University of South Africa, Private Bag X06, Florida 1710, South Africa*

[f] *Botswana University of Agriculture and Natural Resources (BUAN), Gaborone, Botswana*

A R T I C L E I N F O

Keywords:
Calcite nanoparticles
Tomato
Foliar application
Nanofertilizers
Antifungal activity

A B S T R A C T

Bio-synthesized calcium carbonate nanoparticles ($CaCO_3$ NPs) have gained attention because of their cost-effectiveness, minimal toxicity, biological compatibility, cytological compatibility, pH sensitivity, gradual biological degradability and ecological friendliness. As the global population is expected to rise to billions, innovative strategies to enhance crop production are necessary to address poverty challenges. This study assesses the effect of the bioinspired $CaCO_3$ NPs as nanofertilizers on the development, gas exchange and yield parameters of tomatoes (*Lycopersicon esculentum*) and their antifungal activity. The trial was conducted in a 2×4 completely randomised design (CRD) with four replicates. The treatments consisted of different $CaCO_3$ NPs concentrations (Control = 0 mg/L, 50 mg/L, 150 mg/L and 250 mg/L) on two tomato cultivars (Money-maker and Heinz-1370), and the antifungal activity of the $CaCO_3$ NPs was tested against pathogens that cause diseases in tomato plants. The results demonstrate that $CaCO_3$ NPs exhibit moderate antifungal activity against *Cladosporium cladosporioides*, *Fusarium oxysporum* and *Penicillium halotolerans* at minimum inhibitory concentration (MIC) values of 125, 250 and 500 μg/mL. Results further show that 250 mg/L exhibits the highest number of leaves on Money-maker, while 150 mg/L gave the highest number of leaves at week 8 for Heinz-1370. The application of 150 mg/L yielded the highest number of flowers in both cultivars compared to other treatments. Remarkably, different $CaCO_3$ NP concentrations varied the gas exchange parameters and revealed that at concentrations higher than 150 mg/L, the efficiency of water use during the vegetative and fruiting stages was lowered. The highest fruit weight of the Money-maker was observed at 50 mg/L, whereas Heinz-1370's fruit weight was higher at 250 mg/L, indicating that the two cultivars are affected differently by the foliar application of $CaCO_3$ NPs. Therefore, the findings of this study suggest that the inclusion of a green synthesis of $CaCO_3$ NPs as a nanofertilizer has the potential to promote tomato growth and yield.

1. Introduction

The tomato (*Lycopersicon esculentum*) is the second most significant crop after the potato beacause it has enormous economic importance, nutritional value and sensory attributes (Oke et al., 2017). Its fruits contain a variety of minerals and vitamins such as Fe, Mn, Zn and Cu; vitamins C and E; β-carotene; lycopene; flavonoids; organic acids; phenolics; oleic acid; linolenic acid; and chlorophyll (Elbadrawy and Sello,

* Corresponding author at: UNESCO-UNISA Africa Chair in Nanosciences and Nanotechnology, College of Graduates Studies, University of South Africa, Muckleneuk Ridge, Pretoria 392, South Africa.

E-mail address: motlhalammethobo@gmail.com (T. Motlhalamme).

https://doi.org/10.1016/j.plana.2023.100050
Received 10 June 2023; Received in revised form 27 October 2023; Accepted 30 October 2023
Available online 3 November 2023

2016). Tomatoes are consumed in fresh, cooked and processed forms and have been linked to a lowered probability of inflammatory diseases, cancers and chronic non-infectious illnesses (Bilalis et al., 2018; Gorni et al., 2022).

The quantity and quality of plant products are influenced by the soil quality in which agricultural techniques are applied (Oliver and Gregory, 2015). However, soil degradation has led to yield losses of up to 8.2%, particularly in Africa and Asia (Alam, 2014; Eswaran et al., 2019). To mitigate this loss, inorganic fertilisers have been proposed for improved crop quality and yields, which are needed to feed the increasing human population (Bindraban et al., 2015). The increased use of conventional fertilizers has led to water, soil and air pollution through toxic compound accumulation such as heavy metals (Savci, 2012). In addition to soil degradation, fungal diseases are among the prominent factors that negatively affect tomato production and have been responsible for significant losses worldwide due to their resistance to common fungicides (Alam and Ben Hamida, 2014). Therefore, to minimize the depletion of productive lands, maximize the use of remaining land and water, and reduce fungal disease resistance, innovative technologies such as nanotechnology should be implemented (Agrawal and Rathore, 2014; Alam and Ben Hamida, 2014; Duhan et al., 2017).

Agriculture is paying much of attention to nanotechnology. Recent studies have shown that it may benefit the agricultural industry by increasing the effectiveness of agricultural inputs and supplying solutions to agricultural and environmental problems to increase food production and security (Usman et al., 2020). Nanomaterials with specific and unique chemical formulations and physical properties can be used as nanofertilizers, nanopesticides and nanosensors to attain sustainable agriculture practices, thus reducing the harmful effects of fertilizers and pesticides on the environment and untargeted organisms (Amir et al., 2019; Chhipa, 2019). The beneficial effects of nanoparticles on plant development have already been demonstrated, with Hua et al. (2015) reporting yield augmentation in *Citrus tankan* and better control of *Aonidiella aurantia* and *Bactrocera dorsalis* through the application of nano-$CaCO_3$. Similarly, $CaCO_3$ nanoparticles improved the overall performance of groundnuts in a controlled environment (Nelwamondo et al., 2023).

The tomato plant is ranked as one of the most commonly grown staple foods for human consumption in different countries. However, tomato production is altered by multiple external variables including flooding, water scarcity, salinity, high temperatures and pollution (Ojuederie et al., 2019). Moreover, pest and microbial outbreaks are major threats that lead to a decrease in tomato yield (Kolomiets et al., 2017). To protect tomato plants from microbial infections, different types of fungicides and pesticides such as chloroxylenol, phenic methamidophos, chlorpyrifos, methomyl and γ-cyhalothrin, to mention a few, are commonly used and these anti-infectives although effective against microorganisms are harmful to both people and nature (Elgueta et al., 2020). In recent years, innovators in biotechnology have focused on to producing biological techniques for plant defence which are grounded on the manipulation of genetic material, which includes hormonal crosstalk in tomatoes to develop pathogen-resistant plants, however, the development of these methods is expensive (Ortigosa et al., 2019; Rommens and Kishore, 2000) despite continued efforts to minimize the threats that can lead to the reduction of yield in tomatoes. This study envisages that the synthesis of nanoparticles that are categorized by low toxicity and have a broad spectrum of action against tomato fungal pathogens will be a promising method that should be further explored. Thus, this study aims to underline the use of bio-synthesized $CaCO_3$ nanoparticles as nanofertilizers on tomato plants (*Lycopersicon esculentum*) and to assess their antifungal properties against the fungal strains that commonly affect tomato cultivation in addition to their effect on tomato yield.

2. Materials and methods

2.1. Experimental site

The experimentations were carried out at the University of South Africa, at its Florida campus at latitude S26°9.501 and longitude E27°54.113, where the effect of nanoparticles on tomato (*L. esculentum*) plants was tested under glasshouse conditions at the university campus' horticulture centre.

2.2. $CaCO_3$ nanoparticles synthesis

The extract of *Hyphaene thebaica* L. Mart (Egyptian doum palm) fruits was used as the reducing/capping agent for the synthesis of $CaCO_3$ nanoparticles. Immediately after collection, the fruits were cleaned with deionized water and air-dried at room temperature. Three point thirty-two grams (3.32 g) of $CaCl_2$ was mixed with 100 mLof *Hyphaene thebaica* fruit extract under gentle CO_2 bubbling, and the solution was left at ambient temperature for 24 hours. After centrifuging the mixture for 20 min at 4000 rpm and collecting the precipitate, the mixture was washed three times in deionized water and then three times in ethanol. The mixture was centrifuged once again at 4000 rpm for 10 min to allow the precipitate to settle under the tube. Finally, the precipitate was collected and dried at room temperature until a white powder was acquired, which was kept for further characterization and usage.

2.3. Material characterization

The phase and structural identification of the nanoparticles were determined using a multifunctional Bruker AXS (Germany) D8-Advance X-ray diffractometer running at a continuous scan in locked coupled mode with Cu-K radiation (K1 = 1.5406). The parameters were determined within a 2=0.034° range. A Lyn-Eye position-sensitive sensor was used to capture the diffraction data at a typical rate of 0.5 sec per cycle. The modified Scherrer equation $L = \frac{K\lambda}{\beta\cos\theta}$ was used to calculate the nanoparticle crystal size, whereby λ is the X-ray wavelength, β is the peak width at half the maximum weight, and K is the Scherrer constant (0.9) (Monshi et al., 2012). A Field Emission Scanning Electron Microscope (FE-SEM) was used to determine the structure using a beam intensity of 5 KeV. SEM pictures were obtained at a magnification between 10x and 3000x. The elemental composition of the powder samples was determined using a Thermo Fisher Scientific Energy Dispersive Spectrometer (EDS) with a photon energy of 15 KeV and a resolution of 5000x (Orasugh et al., 2020). A Tecnai F20 FEG-TEM microscope in bright field mode at 200 KeV was used to obtain HR-TEM images. The compositional characteristics of the nanopowders were assessed using a Frontier FTIR spectrometer. All FTIR analyses were performed using the Perkin Elmer FTIR in the range of 4000 – 400 cm^{-1} by mixing the powders with dried KBr at room temperature (Arya et al., 2018). The optical properties were then evaluated through a Perkin Elmer Ultraviolet-visible (UV-Vis) Lambda 650 S spectrometer. The measurements were carried out in a wavelength range of 250 nm – 800 nm (Al-Hadeethi et al., 2017).

2.4. Experimental design

The trial was arranged in a 2×4 completely randomised design with four replicates. The treatments included two tomato cultivars (Moneymaker and Heinz-1370) and three concentrations of $CaCO_3$ nanoparticles at 50 mg/L, 150 mg/L and 250 mg/L in a deionized water solution, and a negative control where no nanoparticles were applied. The specific concentrations chosen for this study were recommended in a study by Salcido-Martinez et al. (2020). Foliar application was performed at 10-day intervals. One hundred millilitres (100 mL) of the nanoparticle solution were sprayed onto each tomato plant. A standard calcium-free nutrient solution was evenly applied to all plants and Forteco's profit cocopeat substrate was used as the growth media.

2.5. Plant material source, fungal strains and reagent

The seeds of two tomato cultivars Money-maker and Heinz-1370 were acquired from the Garden World Nursery in Johannesburg, South Africa. The tomatoes were planted in nutrient-free media (cocopeat) purchased from Culterra (Pty) Ltd. Fungal cultures of *Cladosporium cladosporioides* (PPRI 10367), *Fusarium oxysporum* (MRC 1907) and *Penicillium halotolerans* (PPRI 25804) were obtained through Professor Lyndy McGaw from the Phytomedicine Programme at the Department of Paraclinical Sciences at the University of Pretoria's Onderstepoort campus. The potato dextrose agar (PDA), the potato dextrose broth (PDB) media and p-iodonitrotetrazolium violet (INT) were purchased from Sigma-Aldrich (MERCK, South Africa).

2.6. Photosynthetic rates

Three completely grown leaves per replication were used to evaluate gas exchange using the techniques established in the study headed by Gyogluu et al. (2018). A mobile infrared gas analyzer (LI-6400/XT, version 6.2) was used to assess the rates of photosynthetic activity, stomatal conductance, intercellular CO_2 levels, and transpiration. A constant temperature of 25 °C, a CO_2 intensity of 380 µmol/mol, a gas flow of 500 µmol/s, and a photosynthetic photon flux density of 1000 µmolm^{-2}/s were the predominant parameters in the chamber. Measurements were obtained in the morning between 10:00 a.m. and 12:00 p.m. The ratio of photosynthetic rates to stomatal conductance was employed to calculate an instant estimate of water usage efficiency.

2.7. Antifungal activity

The ability of the $CaCO_3$ NPs to inhibit fungi was determined against three fungal species namely, *C. cladosporioides*, *F. oxysporum* and *P. halotolerans* using the minimal inhibitory concentration (MIC) serial microdilution method outlined in Masoko et al. (2007). The fungi were subcultured from potato dextrose agar (PDA) slants on plates of the ready-to-use potato dextrose broth (PDB) growth medium at a constant temperature of 35 ºC for 7 days. After mixing with distilled water to make a stock solution of 5 mg/mL, the CaCO3 NPs were serially diluted two-fold in a 96-well microtitre plate. One hundred microliters (100 µL) of the fungal strains were inoculated into wells containing the test sample and incubated at a constant temperature of 35 ºC for 48 hours. Next, 20 µL of 0.2 mg/mL of p-iodonitrotetrazolium violet (INT) was added to each of the wells. The MIC was recorded through observation as the minimal concentration of $CaCO_3$ NPs that inhibited fungal growth after 48 hrs. An FDA-approved commercial drug, Amphotericin-B, was included as a reference standard, and the experiments were conducted in triplicates with three technical repeats.

2.8. Data collection

The plant's physiological and growth parameters included the plant's height, the number of leaves, branches, flowers, and days to flowering. Additionally, the gas exchange measurements (photosynthetic rate, stomatal conductance, intercellular CO_2 concentration, transpiration efficiency and water use efficiency) were collected during the vegetative and fruiting stages. The fruits' weight and diameters were also recorded.

2.9. Statistical analysis

TIBCO Statistica version 14.0's December 2020 package was used to perform a two-way analysis of variance (ANOVA). Mean separations were done using Fisher's Least Significant Difference (LSD) test at $P<0.05$ with 2 independent variables, namely tomato cultivars and nanoparticle application levels. The dependent variables were plant growth parameters and gas exchange measurements.

3. Results and discussions

3.1. The physical properties of $CaCO_3$ NPs

The X-ray diffractometer (XRD) results presented in Fig. 1(A) show that a crystalline phase of $CaCO_3$ nanoparticles was obtained during the synthesis process. The peaks at 012, 104, 110, 113, 202, 018, 116, 211, 122, 214 and 300 correspond to the rhombohedral calcite phase of $CaCO_3$, which is following with the X-pert standard card #47–1743. This is supported by the results asserted in research by Babou-Kammoe et al. (2012) and Ghiasi and Malekzadeh (2012). The crystalline size was estimated employing the modified Scherrer formula reported by Babou-Kammoe et al. (2012). The average crystalline size of the $CaCO_3$ nanoparticles was ∼61 nm. Sargheini et al. (2012) obtained similar-sized $CaCO_3$ nanoparticles by ball milling method.

The UV-Vis spectrum (Fig. 1D) confirms the synthesis of $CaCO_3$ NPs with the peak showing absorption of light between 300 nm and 400 nm, which is in the range of commercial $CaCO_3$, and with further reference peaks of $CaCO_3$ that absorb light in the wavelength 200–400 nm (Phuong et al., 2021). A band gap energy of 3.30 eV was calculated using the Tauc method, and a range of 3.15–3.36 eV was observed for $CaCO_3$ synthesized using limestone (Ramasamy et al., 2018).

The elemental analysis of $CaCO_3$ nanoparticles performed using Energy Dispersive Spectroscopy (EDS) is presented in Fig. 1(B). The results show that the analyzed powder contains calcium, carbon, oxygen and potassium, thus confirming the XRD results presented in Fig. 1(A). The traces of K in the sample are the result of a high presence of the element in the chemical composition of the plant extracts used (Bahru et al., 2019), however, the prevalent carbon peak is caused by the use of a C coating agent before being injected into the spectrometer to prevent particle charge mechanisms that lead to material deterioration (Viesca et al., 2011). In additionally, the synthesized nanoparticles agglomerated to form a spherical shape shown by SEM imaging in Fig. 2(A). The particles showed a size distribution between 40 nm and 180 nm, however, most particles had a size of less than 120 nm (Fig. 2B).

The FTIR spectrum of the $CaCO_3$ nanoparticles is presented in Fig. 1 (C). Distinct peaks were identified at wavenumbers 711, 876 and 1392 cm^{-1} thus corresponding to the inplane bending, the out-of-plane bending and the asymmetric stretching vibration peaks of calcium carbonate. A sharp peak at 1795 cm^{-1} corresponding to the C=O bond stretching of the acid halide group and a peak at 2508 cm^{-1} corresponding to the O-H stretching of the carboxylic acid, is consistent with the results observed by Garg et al. (2021). Hence, the carbonate ion's symmetric stretch occurs at a wavelength of approximately 1080 cm^{-1}, the out-of-plane bending absorption occurs at a wavelength of ∼870 cm^{-1}, while the asymmetric stretch occurs at a wavelength of approximately 1400 cm^{-1}, and the in-plane bending occurs at a wavelength of around 700 cm^{-1} (Cai et al., 2010).

Fig. 3 shows the TEM imaging and the particle size distribution of the synthesized $CaCO_3$ nanoparticles. The image in Fig. 3(A) shows the different nanoparticle shapes from quasi-spherical, to cubical with equiaxed morphology. The size distribution (see Fig. 3B) shows particle sizes ranging from 60 nm - 180 nm, as confirmed by the SEM results of the present study and the findings reported by Tsuzuki et al. (2000), in which similar particles were obtained through mechanochemical synthesis.

3.2. Antifungal activity

Nanoparticles have demonstrated antimicrobial activity and defence mechanisms against plant diseases (Ali et al., 2020; Hernández-Díaz et al., 2021; Jo et al., 2009; Kaningini et al., 2023). In this study, the

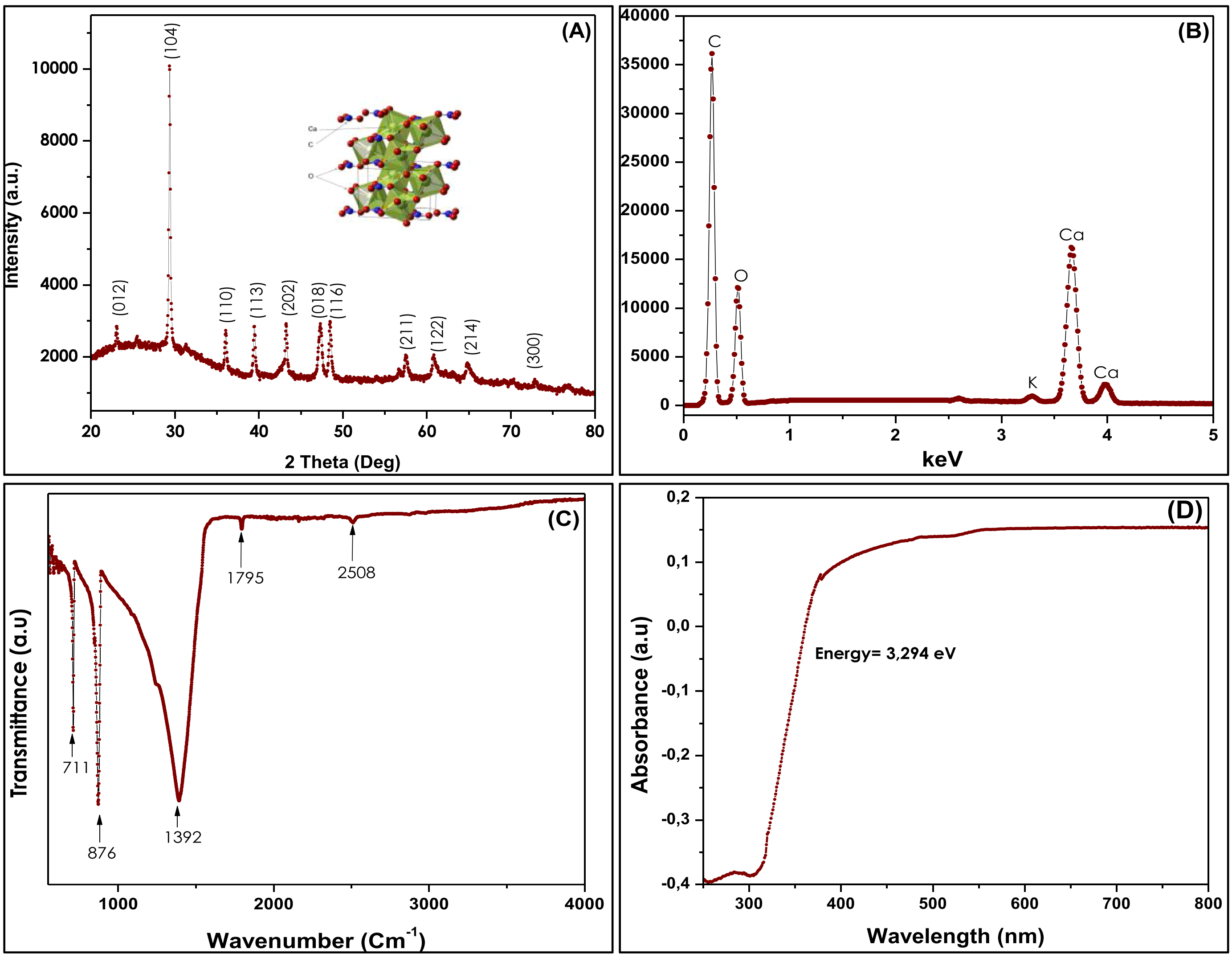

Fig. 1. (A) XRD pattern; (B) EDS; (C) FT-IR; (D) UV-Vis spectra of $CaCO_3$ NPs synthesized through green chemistry utilizing *H. thebaica fruit* extract as the reducing agent.

minimum inhibitory concentration (MIC) representing strong activity was categorised as MIC $\leq$ 31.3 µg/mL, additionally, MIC values of $\leq$ 125 µg/mL were regarded as an indication of effective antifungal action; those between 500 and 250 µg/mL showed moderate activity; and those from 1000 to 500 µg/mL were indicative of weak antifungal activity, as indicated in Table 1. The $CaCO_3$ NPs were considered to have effective antifungal properties with an MIC value of 125 µg/mL against *F. oxysporum*, whereas moderate activity was recorded against *C. cladosporioides* (MIC = 250 µg/mL) and *P. halotolerans* (MIC = 500 µg/mL). The positive control *amphotericin-B* (MIC = 7.8, 15.6, 31.3 µg/mL) had a strong significant inhibitory effect against *C. cladosporioides*, *F. oxysporum* and *P. halotolerans* in the respective order. Dhiman et al. (2022) evaluated the antifungal effect of green synthesized zinc oxide (Tb-ZnO) nanoparticles on *Alternaria brassicae* using different assays including protein, carbohydrates, chitin content and stress enzymes of the fungal cell. Additionally, the Dhiman et al. (2022) study revealed that Tb-ZnO NPs have fungicidal activity, whereas Ataee et al. (2011) demonstrated the antibacterial effect of $CaCO_3$ NPs against *Agrobacterium tumefaciens* using the broth dilution method with a MIC value of 31.2 µg/mL.

3.3. Gas exchange measurements and growth parameters

3.3.1. Gas exchange during vegetative growth

Calcium is a key element in photosynthesis and stomatal regulation. It acts as a cofactor in cell membrane activation. Ca^{2+} ions are mainly located in the chloroplast or the chloroplast membrane, and they affect cytoplasm-regulating pathways (Wang et al., 2019), thus affecting the gas exchange dynamics and photosynthesis capability of cell membranes (Song et al., 2020). The findings in Table 2 demonstrate that the various physiological parameters during the vegetative stage differ significantly from one another. The photosynthetic rate of the Money-maker cultivar (see Fig. 4A) was low in the control treatment and high in plants treated with 50 mg/L (12.28 $\mu molCO_2.m^{-2}.s^{-1}$). For this cultivar, 250 mg/L and the control showed higher stomatal conductance with averages of 0.26 $mmolH_2O.m^{-1}.s^{-1}$ as shown in Fig. 4(B). The highest instantaneous water use efficiency was 79.05 $mmolCO_2.m^{-1}\cdot H_2O$ which was obtained at 150 mg/L. However, when matched with the control, the intercellular CO_2 concentration was reduced with the foliar spray of $CaCO_3$ NPs. In addition, higher values of transpiration were recorded at 250 mg/L and 150 mg/L $CaCO_3$ concentrations. Within the plant system, $CaCO_3$ NPs disintegrate into CO_2 and CaO, which then provide calcium to the plant, hence intensifying photosynthesis (Sorour, 2021).

For the Heinz-1370 cultivar, 250 mg/L had the greatest

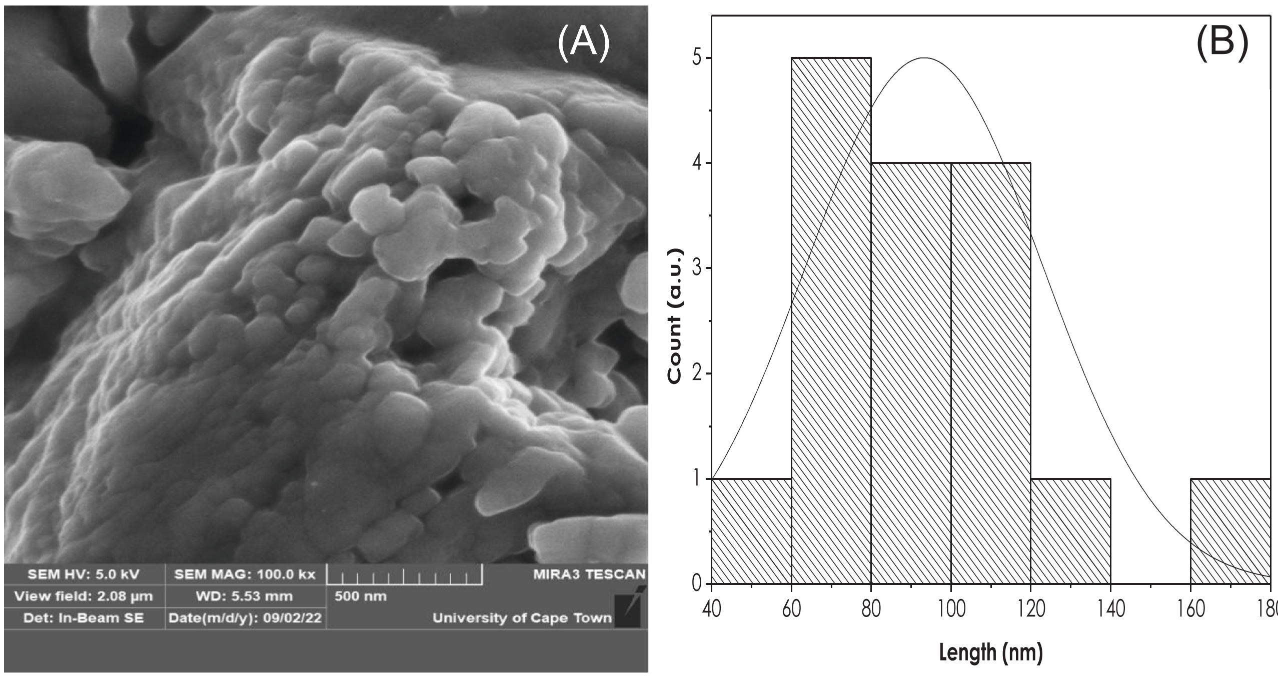

Fig. 2. (A) SEM image obtained at 3.0 kV energy and a magnification of 35000x at 100 nm scale; (B) particle size distribution of $CaCO_3$ nanoparticles.

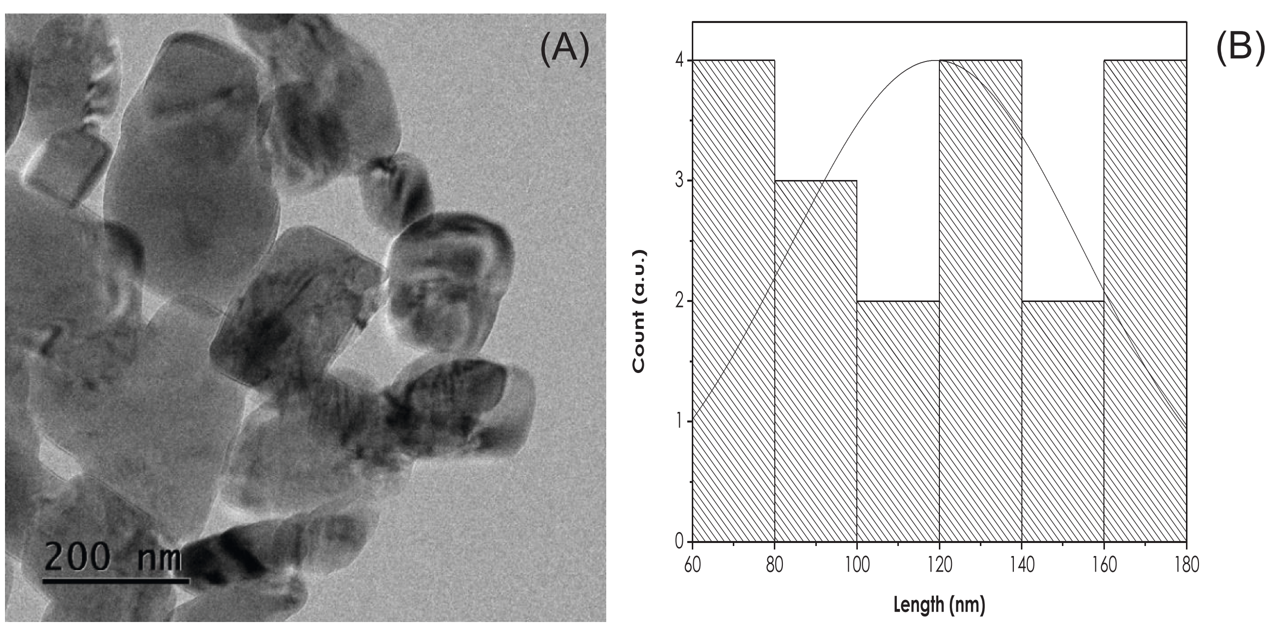

Fig. 3. The (A) transmission electron microscopy micrograph; and (B) particle size distribution of $CaCO_3$ nanoparticles.

Table 1
$CaCO_3$ NPs in-vitro antifungal activity is represented as minimum inhibitory concentration (MIC) values in µg/mL. Independent experiments, n = 3.

	C. cladosporioides	*F. oxysporum*	*P. halotolerans*
$CaCo_3$ NPs	250	125	500
Amphotericin-B	7.8	15.6	31.3

photosynthetic rate at 13,16 µmolCO_2.m^{-2}.s^{-1} and a transpiration rate of 3.09 µmolCO_2molair^{-1}. The stomatal conductance was high on the control treatment which was 0.28 mmolH_2O.m^{-1}.s^{-1}, while the intercellular CO_2 concentration and water use efficiency records were higher at 150 mgL^{-1} with averages of 269.49 mmol.m^{-2}.s^{-1} and 74.44 mmolCO_2.m^{-1}·H_2O, respectively. These results suggest that concentrations of $CaCO_3$ NPs above 150 mgL^{-1} reduce water use efficiency in both cultivars. Plant stomata openings are important in adjusting the circulation of CO_2 and H_2O vapour between the leaves and the atmosphere, while also enhancing photosynthesis and transpiration rate, thus water use efficiency (WUE) is measured at the leaf level (Wei et al., 2018). Furthermore, the treatments had a significant effect on the stomatal conductance (Gs), but the transpiration efficiency (E) was remarkably influenced by the cultivars and treatments. Moreover, intrinsic water use efficiency (WUEi) is significantly influenced by these treatments.

3.3.2. Plant height

The findings presented in Table 3 reveal that the growth parameters

Table 2
Interactive effect of $CaCO_3$ nanoparticles and cultivars on the photosynthetic rate (A); stomatal conductance (Gs); intercellular CO_2 concentration (Ci); transpiration efficiency (E.); water use efficiency (WUE) of L. esculentum.

	A $\mu molCO_2.m^{-2}.s^{-1}$	Gs $mmolH_2O.m^{-1}.s^{-1}$	Ci $mmol.m^{-2}.s^{-1}$	E $\mu molCO_2molair^{-1}$	WUEi $mmolCO_2.m^{-1}\cdot H_2O$
Cultivar					
Money-maker	11.31±0.45a	0.21±0.01a	263.87±4.69a	3.41±0.18a	64.54±3.42a
Heinz-1370	11.94±0.56a	0.24±0.01a	253.46±6.67a	2.88±0.13b	64.59±5.05a
$CaCO_3$ treatments					
50 mg/L	11.87±0.58ab	0.21±0.02 BCE	248.09±10.64a	3.18±0.19ab	66.24±4.99ab
150 mg/L	11.63±0.60ab	0.17±0.01c	261.70±6.61a	3.38±0.15a	76.74±5.32a
250 mg/L	12.56±0.83a	0.26±0.02ab	263.33±7.69a	3.38±0.34a	57.50±4.82b
Control	10.45±0.80b	0.27±0.03a	261.54±7.26a	2.62±0.16b	57.78±8.17b
F Statistics					
Cultivar (C)	0.78 ^{ns}	1.58 ^{ns}	1.63 ^{ns}	5.76***	0.00 ^{ns}
Treatment (T)	1.55 ^{ns}	5.50***	0.76 ^{ns}	2.63***	2.33***
C*T	2.05 ^{ns}	0.75 ^{ns}	1.38 ^{ns}	0.12 ^{ns}	1.80 ^{ns}

Values show the means±standard error; the letters indicate significant differences at *** $p<0.05$, ns= not significant.

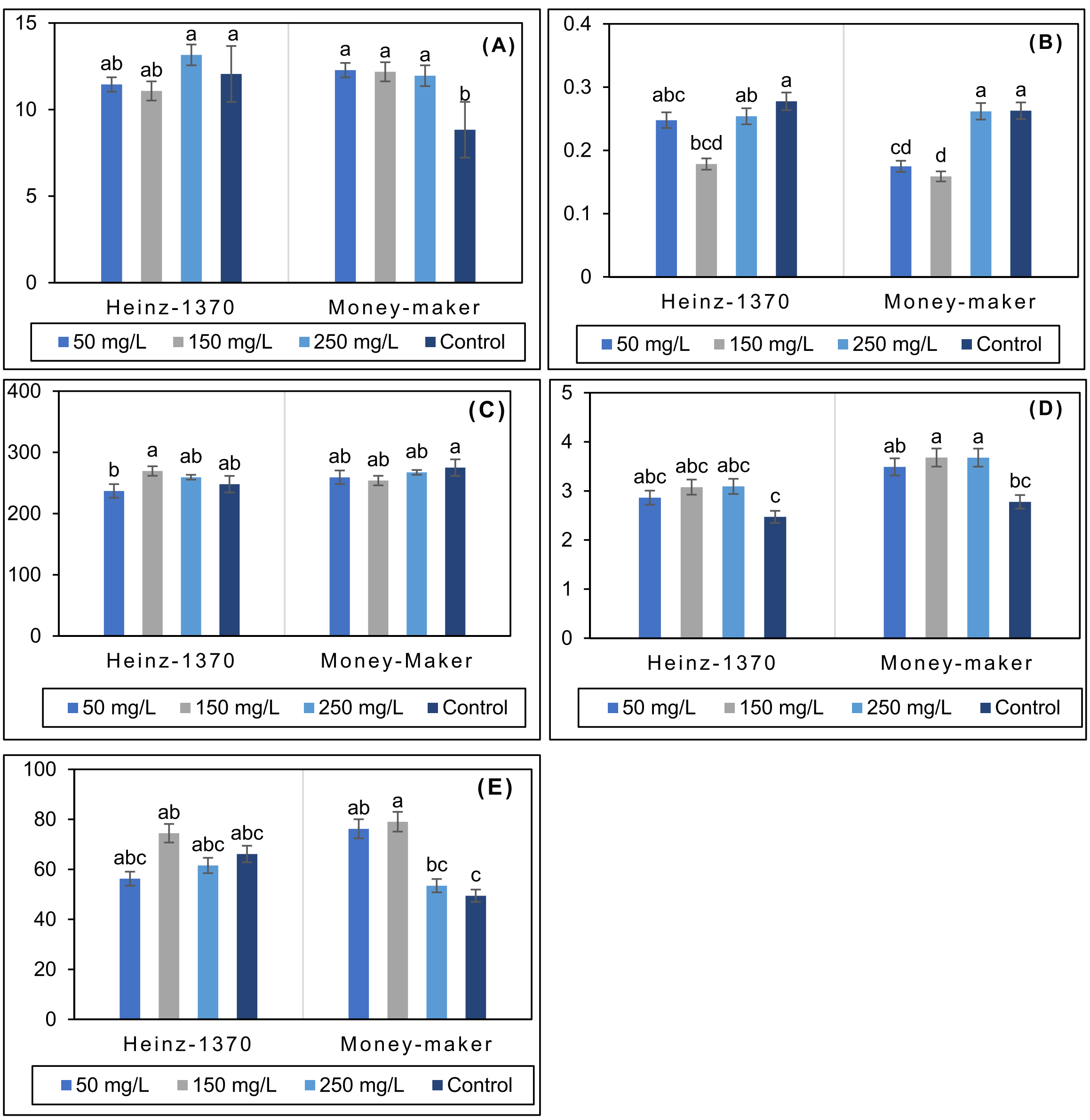

Fig. 4. Interaction effects of cultivars and $CaCO_3$ concentrations on (A) photosynthetic rate; (B) stomatal conductance; (C) intercellular CO_2 concentration; (D) transpiration efficiency; (E) water use efficiency of tomato plants during the vegetative stage under glasshouse conditions. The vertical lines on the bars represent S.E. Bars followed by different letters that are significant at $p \leq 0.05$.

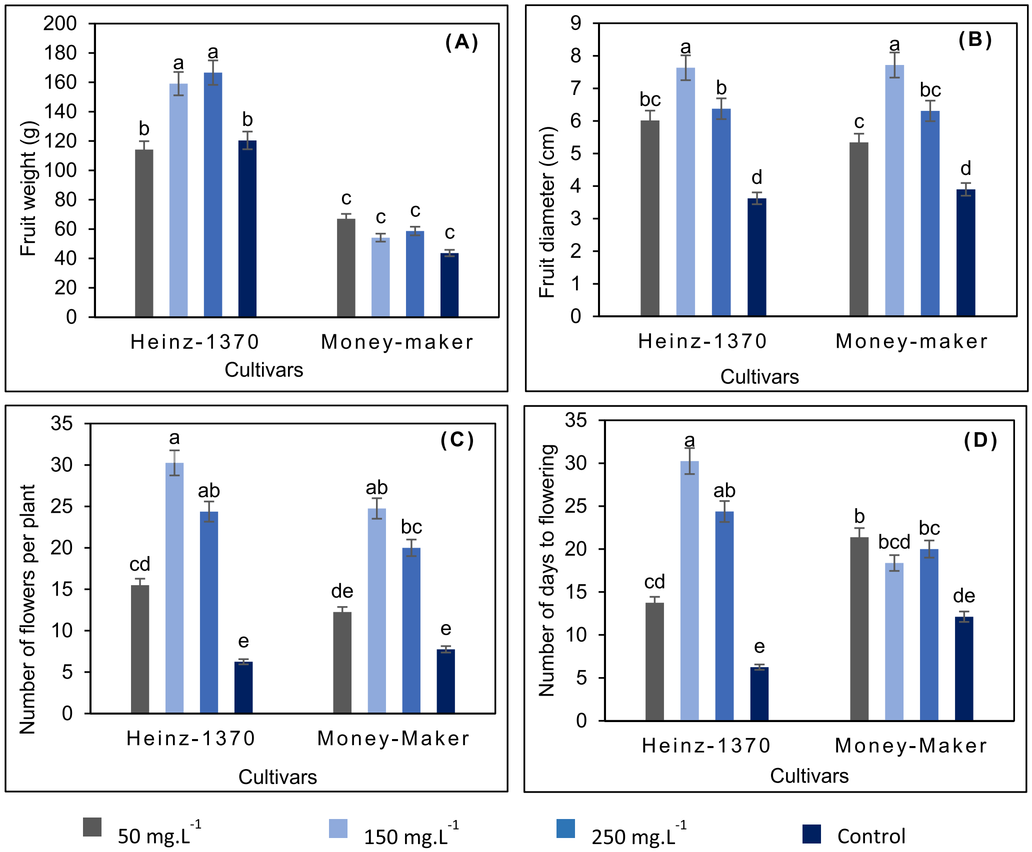

Fig. 5. Summary of the effect of $CaCO_3$ nanoparticles on (A) fruit weight; (B) fruit diameter; (C) number of flowers; (D) days to flowering of L. esculentum. The vertical lines on the bars represent S.E. bars. The different letters indicate significance at $p \leq 0.05$.

Table 3
Effect of cultivars and treatments on the plant height, number of leaves and number of branches of foliar-sprayed tomato plants.

	Plant height		Number of leaves		Number of branches	
	Week 4	Week 8	Week 4	Week 8	Week 4	Week 8
Cultivars						
Money Maker	124.91±7.03a	160.84±5.31a	33.13±1.63b	50.56±1.22b	8.09±0.59b	24.66±1.10b
Heinz 1370	109.59±4.72b	148.63±3.27b	36.97±2.24a	53.44±1.51a	9.56±0.38a	28.81±1.39a
$CaCO_3$ treatments						
50 mg/L	127.94±2.90b	158.63±1.80c	29.56±1.31b	50.19±0.76b	8.19±0.36b	24.75±1.14c
150 mg/L	137.56±4.60a	174.69±4.51a	35.38±1.13a	58.56±1.03a	10.31±0.55a	33.50±1.49a
250 mg/L	138.63±5.57a	168.25±3.51b	38.06±1.82a	58.13±0.89a	10.38±0.87a	29.44±1.65b
Control	64.88±1.69c	117.38±1.43d	37.19±4.85a	41.13±0.54c	6.44±0.53c	19.25±0.64d
F Statistics						
Cultivar (C)	33.67***	43.75***	7.114***	16.34***	6.57***	12.56***
Treatment (T)	178.39***	194.53***	7.04***	133.19***	10.88***	27.40***
C*T	15.58***	22.34***	50.72 ^{ns}	2.73 ^{ns}	1.58 ^{ns}	1.32 ^{ns}

Values show the means±standard error, letters indicate significant differences at *** p<0.05, ns= not significant.

vary remarkably between the two tomato cultivars and across the different concentrations of $CaCO_3$ NPs. Calcium plays an important function in plant development as it is a key element of a cell wall. Additionally, Ca is considered a growth regulator of both the shoots and roots (Hepler, 2005). The money-maker cultivar exhibited the highest plant height with an application of 250 mg/L at week 4, and at week 8, the greatest plant height was recorded with an application of 150 mg/L. However, the plant height records for the Heinz-1370 cultivar were higher with applications of 50 mg/L at week 4 and 150 mg/L at week 8. Increased plant height in response to $CaCO_3$ NPs application correlates with an experiment by Aklog et al. (2016) in which a mixture of proteins, calcium carbonate, and chitin nanofibers made from crab shells increased plant height and the biomass of the tomato plant. It has also been discovered from interactive effect results, that during weeks 4 and 8, all the different variables were significantly influenced by the cultivar, its treatments and the interactions between these aspects.

3.3.3. Number of leaves

The cultivar and its treatments had a significant effect on the number of leaves as shown in Table 3. Money-maker plants sprayed with 250 mg/L had the highest number of leaves in both weeks 4 and 8. The Heinz-1370 cultivar control plants had the highest record of leaves per plant in week 4. At week 8, however, Heinz-1370 plants sprayed with 150 mg/L showed the best performance. These results concur with the conclusions of the study by Aklog et al. (2016), who suggest the positive action of $CaCO_3$ nanoparticles in the promotion of plant development.

Plant cell walls are constructed in part by calcium, which occurs in the form of calcium pectate (Chen et al., 2021), and in addition to acting as a cytosolic transmitter and a vacuolar counteraction for inorganic and organic anions, calcium also plays structural functions in cell membranes and walls (White and Broadley, 2003).

3.3.4. Number of branches

The results show that for both cultivars, the highest number of branches was obtained with the application of 250 mg/L at week 4 and 150 mg/L at week 8, thus demonstrating that $CaCO_3$ NPs can increase the number of branches per plant. Related results were obtained by Elshahawy et al. (2018) using silver nanoparticles (Ag NPs) on tomato plants infected with *Pythium aphanidermatum*. Moreover, treating strawberry plants affected by *Botrytis cinerea* with $CaCO_3$ and Fe_2O_3 (Iron III Oxide) nanoparticles had a favourable impact on the stimulation of plant development (Mogazy et al., 2022). However, Younes and Nassef (2015) showed that the application of Ag NPs to salt-stressed tomato plants resulted in a reduction in the quantity of fruits produced per plant, the size of the fruits, the weight of the typical fruit, the number of branches per plant, and the height of the plant.

3.3.5. Gas exchange measurements during fruiting

The interactive effects results for the gas exchange measurements reveal that the cultivar, treatment and C*T combination have no significant effect on any of the gas exchange parameters (see Table 4). Furthermore, the observed measurements reveal that the money-maker had the highest photosynthetic rate and water use efficiency at 150 mg/L. Similar findings were observed for the stomatal conductance between plants sprayed with 50 mg/L and the control treatment, however, the highest intercellular CO_2 concentration was observed in the control plant, while the transpiration efficiency was higher with the leaves spray of 50 mg/L. In contrast, the highest photosynthetic rate for Heinz-1370 was observed in its control plants, and the highest water use efficiency was observed at an application of 250 mg/L. Tomato cultivars are thought to respond differently to various nutrients and conditions (Olaniyi et al., 2010) and these changing variables allow the relationship between water use efficiency and stomatal conductance to become apparent. Previous research has proven that utilizing nanoparticles can promote plant growth and photosynthetic efficiency (Cao et al., 2017; Hernández-Hernández et al., 2018; Lowry et al., 2019). For instance, ZnO nanoparticles applied at concentrations of 8 mg/L increased these two parameters, in addition to carbonic anhydrase and antioxidants (Faizan et al., 2018). Additionally, the chlorophyll content of tomatoes can be increased by nanoparticle application, hence improving plant photosynthesis (Saffan et al., 2022).

3.4. Yield parameters

3.4.1. Fruit weight and diameter

Significant variations were observed in tomato fruit weight and diameter between the cultivars, and among the various $CaCO_3$ NP concentrations (see Fig. 4A and B). The results demonstrated that the highest fruit weight of 67.00 g in the Money-maker cultivar was acquired with an application of 50 mg/L, while the control had the lowest fruit weight with an average of 43.67 g. For Heinz-1370, the highest fruit weight average of 166.58 g was recorded on 250 mg/L treated plants. Similar trends were shown in a research by Shankramma et al. (2016) which stated an improvement in seedling growth when subjected to a foliar application of 50 mg/L of Fe_2O_3 NPs. Hence, Teixeira et al. (2022) concluded that calcium carbonate nanoparticles can protect and enhance the quality of pineapples, which agrees with the findings of this study on the Heinz-1370 cultivar.

As presented in Fig. 4(B), the application of 150 mg/L exhibited the greatest fruit diameter in both cultivars, with averages of 7.72 cm in Money-maker and 7.63 cm in Heinz-1370. This finding corresponds to that of Vidak et al. (2021), who reported that tomato fruit size can be enhanced by the foliar application,n of calcite. When copper nanoparticles (Cu NPs) were used, similar outcomes were shown with an increase of up to 21% in yield per tomato plant (Hernández-Hernández et al., 2019). Foliar fertilization with nanoparticles could be an efficient way to provide nutrients for quick uptake and use by plants. This is validated by the enhancement of fruit weight and size observed in this study. Therefore, the inclusion of nanoparticles could be an important part of strategies for managing crops to the maximization of crop yield and quality (Haytova, 2013).

3.4.2. Number of flowers and days to flowering

The impacts of the various CaCO3 NP concentrations were evaluated in this study, and the cultivars and nanoparticle concentrations showed a large discrepancy (see Table 5). Applying 150 mg/L resulted in more flowers per plant, for both cultivars, with averages of 30.25 (Money-maker) and 25.75 (Heinz-1370) flowers per plant. The control plants gave the least number of flowers which demonstrates that the incorporation of calcium carbonate nanoparticles affects the number of flowers. This is consistent with findings from research by Siddiqui et al. (2015), where multiwalled carbon nanotubes (MWCNTs) were found to enhance the number of flowers in tomato plants.

According to the results in Fig. 4(D), the rate of flowering is influenced by different concentrations of $CaCO_3$ NPs. Moreover, the control treatment took the longest number of days to flower when contrasted to other treatments across both cultivars. On average, tomato plants sprayed with 150 mg/L had flowers on day 18, while those treated with 250 mg/L flowered on day 20, with control plants taking 23 days to flower on average. The findings imply that the use of $CaCO_3$ NPs

Table 4
The interactive effect of cultivars and $CaCO_3$ treatments on the photosynthetic rate (A); stomatal conductance (Gs); intercellular CO_2 concentration (Ci); transpiration efficiency (E.); water use efficiency (WUEi) of L. esculentum during the fruiting stage.

	A $\mu molCO_2.m^{-2}.s^{-1}$	Gs $mmolH_2O.m^{-1}.s^{-1}$	Ci $mmol.m^{-2}.s^{-1}$	E $\mu molCO_2 molair^{-1}$	WUEi $mmolCO_2.m^{-1}\cdot H_2O$
Cultivars					
Money Maker	16.87±0.45a	0.19±0.01a	246.47±3.34a	2.62±0.15a	132.38±11.57a
Heinz 1370	16.37±0.46a	0.17±0.01a	248.16±3.99a	2.38±0.11a	118.01±7.86a
$CaCO_3$ treatments					
50 mgL^{-1}	16.71±0.56a	0.20±0.02a	249.58±5.60a	2.74±0.17a	106.66±13.24a
150 mgL^{-1}	16.90±0.65a	0.17±0.02a	247.78±5.35a	2.38±0.19a	143.86±16.34a
250 mgL^{-1}	15.90±0.58a	0.16±0.02a	241.55±4.76a	2.27±0.19a	130.02±12.14a
Control	16.97±0.79a	0.19±0.02a	250.35±5.11a	2.59±0.19a	120.24±13.72a
F Statistics					
Cultivar (C)	0.610^{ns}	1.0278^{ns}	0.104^{ns}	1.6979^{ns}	1.0586^{ns}
Treatment (T)	0.585^{ns}	1.0433^{ns}	0.576^{ns}	1.2928^{ns}	1.2634^{ns}
C*T	1.663^{ns}	0.7491^{ns}	0.566^{ns}	0.3705^{ns}	0.8267^{ns}

Values show the means±standard error, letters indicate significant differences at *** $p<0.05$, ns= not significant.

Table 5
The interactive effect of tomato cultivars and their treatments on the number of flowers, days to flowering, fruit weight and fruit diameter.

	Number of flowers	Days to flowering	Fruit diameter (cm)	Fruit weight (g.pant^{-1})
Cultivars				
Money Maker	16.19±1.56a	22.09±0.93a	5.82±0.39a	55.88±3.84b
Heinz 1370	19.09±2.04a	22.78±0.72a	5.91±0.40a	140.06 ±9.04a
Treatments				
50 mg/L	13.88±1.57c	21.31±0.47b	5.68±0.28b	90.58 ±13.27ab
150 mg/L	27.50±1.93a	19.13±0.45c	7.68±0.15a	106.63 ±20.29a
250 mg/L	22.19±1.57b	20.63±1.13 BCE	6.34±0.30b	112.63 ±21.82a
Control	7.00±1.67d	28.69±0.64a	3.76±0.18c	82.04 ±16.64b
F-Statistics				
Cultivar	3.03 ^{ns}	0.86 ^{ns}	0.16 ^{ns}	100.45***
Treatments	29.31***	33.07***	45.63***	2.82***
C*T	0.85 ^{ns}	0.30 ^{ns}	0.73 ^{ns}	2.85***

Values show the means±standard error, letters indicate significant differences at ***$p<0.05$, ns= not significant.

shortens the number of days to flowering. These finding concurs with a study by Byczyńska et al. (2019), who observed that Ag NPs shortened the production cycle of tulips without altering the quality of the plant and its produce.

4. Conclusion

Highly crystalline quasi-spherical $CaCO_3$ NPs with a mean size of 6.9 nm were acquired from the synthesis process using *H. thebaica* fruit extract as a reducing agent. The $CaCO_3$ NPs exhibited moderate antifungal activity against *C. cladosporioides*, *F. oxysporum* and *P. halotolerans*, with minimum inhibitory concentration (MIC) values of 250, 125 and 500 µg/mL. However, *F. oxysporum* is the most susceptible fungal strain to $CaCO_3$ NPs. Prospectively the authors of the study desire to correlate these results using other methods such as time-kill assays to confirm this fungicidal action. Furthermore, tomato biomass production increased through the application of 250 mg/L $CaCO_3$ NPs for Moneymaker and 150 mg/L for Heinz-1370, when contrasted with the control treatments. Flowering in both tomato cultivars was enhanced by the application of 150 mg/L. Fruit yield improved at 50 mgL^{-1} for the Money-maker cultivar, whereas enhancement for Heinz-1370 was achieved at 250 mgL^{-1} $CaCO_3$ NPs. The two cultivars respond differently to various concentrations of $CaCO_3$ NPs due to their genetic makeup. Therefore, this should be considered when making nanoparticle dosage recommendations. The instantaneous water use efficiency was lowered by higher concentrations of $CaCO_3$ NPs during the vegetative and fruiting stages. While the incorporation of $CaCO_3$ nanoparticles in cropping systems for Ca fertilization is ideal for sustainable tomato production, trials should be conducted where plants are inoculated with pathogens to test the efficiency of $CaCO_3$ NPs on the infested plants. Furthermore, their antifungal properties could play a role in crop protection by suppressing fungal diseases in tomato plants. Moreover, this study could provide solutions to reduce the cost of synthesis of nanofertilizers and harmful chemicals in agriculture by using plant materials, in addition to providing solutions to agricultural challenges, which include productivity loss imposed by pests, global climate change effects and the reduction of soil fertility.

Funding statement

The National Research Foundation (TWAS-NRF) of South Africa provided funding for this project (Grant number: 138598).

CRediT authorship contribution statement

Thobo Motlhalamme: Conceptualization, design and execution of experiments; analysis and interpretation of data; writing of the original document. **Hamza Mohamed:** Synthesis of nanoparticles. **Amani Gabriel Kaningini:** Data analysis and draft edition. **Garland Kgosi More:** Antifungal experiments and manuscript editing. Keletso Cecilia Mohale: Manuscript revision and funding. **Force Tefo Thema:** Manuscript revision. **Malik Maaza:** Manuscript revision and funding.

Declaration of Competing Interest

The authors declare the following financial interests/personal relationships which may be considered as potential competing interests: Thobo Motlhalamme reports financial support was provided by National Research Foundation. If there are other authors, they declare that they have no known competing financial interests or personal relationships that could have appeared to influence the work reported in this paper.

Data availability

No data was used for the research described in the article.

Acknowledgements

Much appreciation goes to the Horticulture Center (Unisa Florida Campus) for making its facilities available to us. To Prof. Dakora and Mr Ngmenzuma, thank you so much for your help with the infrared gas analyzer.

References

Agrawal, S., Rathore, P., 2014. Nanotechnology pros and cons to agriculture: a review. Int. J. Curr. Microbiol. App. Sci. 3, 43–55.

Aklog, Y.F., Egusa, M., Kaminaka, H., Izawa, H., Morimoto, M., Saimoto, H., Ifuku, S., 2016. Protein/CaCO3/chitin nanofiber complex prepared from crab shells by simple mechanical treatment and its effect on plant growth. Int. J. Mol. Sci. 17, 1600.

Alam, A., 2014. Soil degradation: a challenge to sustainable agriculture. Int. J. Sci. Res. Agric. Sci. 1, 52.

Alam, M.M., Ben Hamida, E., 2014. Surveying wearable human assistive technology for life and safety critical applications: standards, challenges and opportunities. Sensors 14, 9153–9209.

Al-Hadeethi, Y., Umar, A., Ibrahim, A.A., Al-Heniti, S.H., Kumar, R., Baskoutas, S., Raffah, B.M., 2017. Synthesis, characterization and acetone gas sensing applications of Ag-doped ZnO nanoneedles. Ceram. Int. 43, 6765–6770.

Ali, M.A., Ahmed, T., Wu, W., Hossain, A., Hafeez, R., Islam Masum, M.M., Wang, Y., An, Q., Sun, G., Li, B., 2020. Advancements in plant and microbe-based synthesis of metallic nanoparticles and their antimicrobial activity against plant pathogens. Nanomaterials 10, 1146.

Amir, L., Maryam, B., Anvar, G., Meisam, Z., 2019. The role of nanotechnology for improving crop production. Вестник Российского университета друЖбы народов. Серия: АгроноМия и Животноводство 14, 297–305.

Arya, A., Gupta, K., Chundawat, T.S., Vaya, D., 2018. Biogenic synthesis of copper and silver nanoparticles using green alga Botryococcus braunii and its antimicrobial activity. Bioinorg. Chem. Appl. 2018.

Ataee, R.A., Derakhshanpour, J., Mehrabi Tavana, A., Eydi, A., 2011. Antibacterial effect of calcium carbonate nanoparticles on Agrobacterium tumefaciens. J. Mil. Med. 13, 65–70.

Babou-Kammoe, R., Hamoudi, S., Larachi, F., Belkacemi, K., 2012. Synthesis of CaCO3 nanoparticles by controlled precipitation of saturated carbonate and calcium nitrate aqueous solutions. Can. J. Chem. Eng. 90, 26–33.

Bahru, T.B., Tadele, Z.H., Ajebe, E.G., 2019. A review on avocado seed: functionality, composition, antioxidant and antimicrobial properties. Chem. Sci. Int. J. 27, 1–10.

Bilalis, D., Krokida, M., Roussis, I., Papastylianou, P., Travlos, I., Cheimona, N., Dede, A., 2018. Effects of organic and inorganic fertilization on yield and quality of processing tomato (Lycopersicon esculentum Mill.). Folia Hortic. 30, 321–332.

Bindraban, P.S., Dimkpa, C., Nagarajan, L., Roy, A., Rabbinge, R., 2015. Revisiting fertilisers and fertilisation strategies for improved nutrient uptake by plants. Biol. Fertil. Soils 51, 897–911.

Byczyńska, A., Zawadzińska, A., Salachna, P., 2019. Silver nanoparticles preplant bulb soaking affects tulip production. Acta Agric. Scand., Sect. B—Soil Plant Sci. 69, 250–256.

Cai, G.-B., Chen, S.-F., Liu, L., Jiang, J., Yao, H.-B., Xu, A.-W., Yu, S.-H., 2010. 1, 3-Diamino-2-hydroxypropane-N, N, N′, N′-tetraacetic acid stabilized amorphous

calcium carbonate: Nucleation, transformation and crystal growth. CrystEngComm 12, 234–241.
Cao, Z., Stowers, C., Rossi, L., Zhang, W., Lombardini, L., Ma, X., 2017. Physiological effects of cerium oxide nanoparticles on the photosynthesis and water use efficiency of soybean (Glycine max (L.) Merr.). Environ. Sci. Nano 4, 1086–1094.
Chen, Y., Li, W., Turner, J.A., Anderson, C.T., 2021. PECTATE LYASE LIKE12 patterns the guard cell wall to coordinate turgor pressure and wall mechanics for proper stomatal function in Arabidopsis. Plant Cell 33, 3134–3150.
Chhipa, H., 2019. Applications of nanotechnology in agriculture. Methods in Microbiology. Elsevier, pp. 115–142.
Dhiman, S., Varma, A., Prasad, R., Goel, A., 2022. Mechanistic insight of the antifungal potential of green synthesized zinc oxide nanoparticles against Alternaria brassicae. J. Nanomater. 2022.
Duhan, J.S., Kumar, R., Kumar, N., Kaur, P., Nehra, K., Duhan, S., 2017. Nanotechnology: the new perspective in precision agriculture. Biotechnol. Rep. 15, 11–23.
Elbadrawy, E., Sello, A., 2016. Evaluation of nutritional value and antioxidant activity of tomato peel extracts. Arab. J. Chem. 9, S1010–S1018.
Elgueta, S., Valenzuela, M., Fuentes, M., Meza, P., Manzur, J.P., Liu, S., Zhao, G., Correa, A., 2020. Pesticide residues and health risk assessment in tomatoes and lettuces from farms of metropolitan region Chile. Molecules 25, 355.
Elshahawy, I., Abouelnasr, H.M., Lashin, S.M., Darwesh, O.M., 2018. First report of Pythium aphanidermatum infecting tomato in Egypt and its control using biogenic silver nanoparticles. J. Plant Prot. Res 58.
Eswaran, H., Lal, R., Reich, P.F., 2019. Land degradation: an overview. Response Land Degrad. 20–35.
Faizan, M., Faraz, A., Yusuf, M., Khan, S.T., Hayat, S., 2018. Zinc oxide nanoparticle-mediated changes in photosynthetic efficiency and antioxidant system of tomato plants. Photosynthetica 56, 678–686.
Garg, Rajni, Kumari, M., Kumar, M., Dhiman, S., Garg, Rishav, 2021. Green synthesis of calcium carbonate nanoparticles using waste fruit peel extract. Mater. Today Proc. 46, 6665–6668.
Ghiasi, M., Malekzadeh, A., 2012. Synthesis of CaCO3 nanoparticles via citrate method and sequential preparation of CaO and Ca (OH) 2 nanoparticles. Cryst. Res. Technol. 47, 471–478.
Gorni, P.H., de Lima, de Oliveira Pereira, G.R., Spera, L.M., de Marcos Lapaz, K.D., Pacheco, A.C, A., 2022. Increasing plant performance, fruit production and nutritional value of tomato through foliar applied rutin. Sci. Hortic. 294, 110755.
Gyogluu, C., Mohammed, M., Jaiswal, S.K., Kyei-Boahen, S., Dakora, F.D., 2018. Assessing host range, symbiotic effectiveness, and photosynthetic rates induced by native soybean rhizobia isolated from Mozambican and South African soils. Symbiosis 75, 257–266.
Haytova, D., 2013. A review of foliar fertilization of some vegetables crops. Annu. Res. Rev. Biol. 455–465.
Hepler, P.K., 2005. Calcium: a central regulator of plant growth and development. Plant Cell 17, 2142–2155.
Hernández-Díaz, J.A., Garza-García, J.J.O., Zamudio-Ojeda, A., León-Morales, J.M., López-Velázquez, J.C., García-Morales, S., 2021. Plant-mediated synthesis of nanoparticles and their antimicrobial activity against phytopathogens. J. Sci. Food Agric. 101, 1270–1287.
Hernández-Hernández, H., González-Morales, S., Benavides-Mendoza, A., Ortega-Ortiz, H., Cadenas-Pliego, G., Juárez-Maldonado, A., 2018. Effects of chitosan–PVA and Cu nanoparticles on the growth and antioxidant capacity of tomato under saline stress. Molecules 23, 178.
Hernández-Hernández, H., Quiterio-Gutiérrez, T., Cadenas-Pliego, G., Ortega-Ortiz, H., Hernández-Fuentes, A.D., Cabrera de la Fuente, M., Valdés-Reyna, J., Juárez-Maldonado, A., 2019. Impact of selenium and copper nanoparticles on yield, antioxidant system, and fruit quality of tomato plants. Plants 8, 355.
Hua, K.-H., Wang, H.-C., Chung, R.-S., Hsu, J.-C., 2015. Calcium carbonate nanoparticles can enhance plant nutrition and insect pest tolerance. J. Pest. Sci. 40, 208–213.
Jo, Y.-K., Kim, B.H., Jung, G., 2009. Antifungal activity of silver ions and nanoparticles on phytopathogenic fungi. Plant Dis. 93, 1037–1043.
Kaningini, A.G., Motlhalamme, T., More, G.K., Mohale, K.C., Maaza, M., 2023. Antimicrobial, antioxidant, and cytotoxic properties of biosynthesized copper oxide nanoparticles (CuO-NPs) using Athrixia phylicoides DC. Heliyon 9.
Kolomiets, J.V., Grygoryuk, I.P., Butsenko, L.M., 2017. Bacterial diseases of tomato plants in terms of open and covered growing of Ukraine. Ann. Agrar. Sci. 15, 213–216.
Lowry, G.V., Avellan, A., Gilbertson, L.M., 2019. Opportunities and challenges for nanotechnology in the agri-tech revolution. Nat. Nanotechnol. 14, 517–522.
Masoko, P., Picard, J., Eloff, J.N., 2007. The antifungal activity of twenty-four southern African Combretum species (Combretaceae). South Afr. J. Bot. 73, 173–183.
Mogazy, A.M., Mohamed, H.I., El-Mahdy, O.M., 2022. Calcium and iron nanoparticles: a positive modulator of innate immune responses in strawberry against botrytis cinerea. Process Biochem. 115, 128–145.
Monshi, A., Foroughi, M.R., Monshi, M.R., 2012. Modified Scherrer equation to estimate more accurately nano-crystallite size using XRD. World J. Nano Sci. Eng. 2, 154–160.
Nelwamondo, A.M., Kaningini, A.G., Ngmenzuma, T.Y., Maseko, S.T., Maaza, M., Mohale, K.C., 2023. Biosynthesis of magnesium oxide and calcium carbonate nanoparticles using Moringa oleifera extract and their effectiveness on the growth, yield and photosynthetic performance of groundnut (Arachis hypogaea L.) genotypes. Heliyon.
Ojuederie, O.B., Olanrewaju, O.S., Babalola, O.O., 2019. Plant growth promoting rhizobacterial mitigation of drought stress in crop plants: Implications for sustainable agriculture. Agronomy 9, 712.
Oke, M.O., Hussein, J.B., Oriola, K.O., Bolarinwa, I.F., 2017. Post-harvest processing and preservative technology of tomato–a review. Int. J. Org. Agric. Res. Dev. 14, 42–71.
Olaniyi, J.O., Akanbi, W.B., Adejumo, T.A., Akande, O.G., 2010. Growth, fruit yield and nutritional quality of tomato varieties. Afr. J. Food Sci. 4, 398–402.
Oliver, M.A., Gregory, P.J., 2015. Soil, food security and human health: a review. Eur. J. Soil Sci. 66, 257–276.
Orasugh, J.T., Ghosh, S.K., Chattopadhyay, D., 2020. Nanofiber-reinforced biocomposites. Fiber-Reinforced Nanocomposites: Fundamentals and Applications. Elsevier, pp. 199–233.
Ortigosa, A., Gimenez-Ibanez, S., Leonhardt, N., Solano, R., 2019. Design of a bacterial speck resistant tomato by CRISPR/Cas9–mediated editing of Sl JAZ 2. Plant Biotechnol. J. 17, 665–673.
Phuong, D.N., Chi, N.K., Le Minh, T., Luat, H.H., Truyen, C.Q., Lam, T.D., 2021. Preparation of CaCO3 nano and microparticles from phosphogypsum of Dinh Vu DAP plant, Viet Nam. Vietnam J. Chem. 59, 440–445.
Ramasamy, V., Anand, P., Suresh, G., 2018. Synthesis and characterization of polymer-mediated CaCO3 nanoparticles using limestone: a novel approach. Adv. Powder Technol. 29, 818–834.
Rommens, C.M., Kishore, G.M., 2000. Exploiting the full potential of disease-resistance genes for agricultural use. Curr. Opin. Biotechnol. 11, 120–125.
Saffan, M.M., Koriem, M.A., El-Henawy, A., El-Mahdy, S., El-Ramady, H., Elbehiry, F., Omara, A.E.-D., Bayoumi, Y., Badgar, K., Prokisch, J., 2022. Sustainable production of tomato plants (Solanum lycopersicum L.) under low-quality irrigation water as affected by bio-nanofertilizers of selenium and copper. Sustainability 14, 3236.
Salcido-Martinez, A., Sanchez, E., Licon-Trillo, L.P., Perez-Alvarez, S., Palacio-Marquez, A., Amaya-Olivas, N.I., Preciado-Rangel, P., 2020. Impact of the foliar application of magnesium nanofertilizer on physiological and biochemical parameters and yield in green beans. Not. Bot. Horticult. Agrobot. Cluj. Napoca 48, 2167–2181.
Sargheini, J., Ataie, A., Salili, S.M., Hoseinion, A.A., 2012. One-step facile synthesis of CaCO3 nanoparticles via mechano-chemical route. Powder Technol. 219, 72–77.
Savci, S., 2012. Investigation of effect of chemical fertilizers on environment. Apcbee Procedia 1, 287–292.
Shankramma, K., Yallappa, S., Shivanna, M.B., Manjanna, J., 2016. Fe 2 O 3 magnetic nanoparticles to enhance S. lycopersicum (tomato) plant growth and their biomineralization. Appl. Nanosci. 6, 983–990.
Siddiqui, M.H., Al-Whaibi, M.H., Firoz, M., Al-Khaishany, M.Y., 2015. Role of nanoparticles in plants. Nanotechnol. Plant Sci. 19–35.
Song, Q., Liu, Y., Pang, J., Yong, J.W.H., Chen, Y., Bai, C., Gille, C., Shi, Q., Wu, D., Han, X., 2020. Supplementary calcium restores peanut (Arachis hypogaea) growth and photosynthetic capacity under low nocturnal temperature. Front. Plant Sci. 10, 1637.
Sorour, M.A., 2021. Enhancing Cycas revoluta Thunb. growth by calcium carbonate nanoparticles under water deficit stress condition. Sci. J. Flowers Ornam. Plants 8, 39–54.
Teixeira, G.C.M., Junior, J.S.P., Mattiuz, B.-H., de Mello Prado, R., Corrêa, A.J., Rocha, A.M.S., do Vale, D.W., 2022. Spraying of calcium carbonate nanoparticles in pineapple fruit reduces sunburn damages. South Afr. J. Bot. 148, 643–651.
Tsuzuki, T., Pethick, K., McCormick, P.G., 2000. Synthesis of CaCO3 nanoparticles by mechanochemical processing. J. Nanopart. Res. 2, 375–380.
Usman, M., Farooq, M., Wakeel, A., Nawaz, A., Cheema, S.A., ur Rehman, Ashraf, H., Sanaullah, M, I., 2020. Nanotechnology in agriculture: Current status, challenges and future opportunities. Sci. Total Environ. 721, 137778.
Vidak, M., Lazarević, B., Petek, M., Gunjača, J., Šatović, Z., Budor, I., Carović-Stanko, K., 2021. Multispectral Assessment of Sweet Pepper (Capsicum annuum L.) Fruit Quality Affected by Calcite Nanoparticles. Biomolecules 11, 832.
Viesca, J.L., Battez, A.H., González, R., Chou, R., Cabello, J.J., 2011. Antiwear properties of carbon-coated copper nanoparticles used as an additive to a polyalphaolefin. Tribol. Int. 44, 829–833.
Wang, Q., Yang, S., Wan, S., Li, X., 2019. The significance of calcium in photosynthesis. Int. J. Mol. Sci. 20, 1353.
Wei, Z., Du, T., Li, X., Fang, L., Liu, F., 2018. Simulation of stomatal conductance and water use efficiency of tomato leaves exposed to different irrigation regimes and air CO2 concentrations by a modified “Ball-Berry” model. Front Plant Sci. 9, 445.
White, P.J., Broadley, M.R., 2003. Calcium in plants. Ann. Bot. 92, 487–511.
Younes, N.A., Nassef, D.M., 2015. Effect of silver nanoparticles on salt tolerancy of tomato transplants (Solanum lycopersicom L. Mill.). Assiut J. Agric. Sci. 46, 76–85.